A Beam Splitter in the $60 \div 210\mu m$ band for PACS calibration

L. Morbidelli[1],

[1]**Istituto di Radioastronomia**

IRA - INAF Technical Report

Abstract

In the present report we perform the necessary calculations in order to obtain the transmission/reflection coefficients of a mylar film in the FIR band of $50 \div 250 \mu m$*. The purpose is to find the best tickness for the film to be used to build a Beam Splitter. This is part of the equipment necessary to perform the calibration of the PACS Photometer/Spectrometer detector, one of the instrument of the ESA Herschel project.*

1 Introduction

Work is in progress by ESA to build and launch a satellite for astronomical observation in the far infrared. The satellite is dubbed **Herschel** (formerly known as **FIRST**) and the launch is foreseen for the year 2008.

It will be deployed in orbit at the Lagrangian point L2 of the Earth/Moon-Sun system, in order to reduce at the smallest possible level the thermal radiation from Earth, and will carry on board three instruments to be able to observe the sky between 60 and 600 μm.

One of the three instrument is PACS (Photoconductor Array Camera & Spectrometer) which will be able to perform photometric and spettroscopic observations in the band $60 \div 210 \mu m$.

- Spettroscopy

  Two $Ge : Ga$ photoconductor arrays *stressed/unstressed* will be used as detectors in this observing mode. Array size is 25×16, at a working temperature of $1.7K$. Field of view is $50'' \times 50''$ with a resolution of about $175 km/s$.

  The *unstressed* array will observe the band $60 \div 120 \mu m$.

  The *stressed* array will observe the $120 \div 210 \mu m$ band.

- Photometry

  In this observing mode two bolometr arrays will be used, one with 64×32 and a second with 32×16 pixels, working at $0.3K$ and with a field of view of $1.75' \times 3.5'$.

  The first array will provide imaging in the $60 \div 90 \mu m$ or $90 \div 130 \mu m$ band.

  The second will image the $130 \div 210 \mu m$ band.

Three instrument are going to be built, respectively called *demonstration, qualification* and *flight model.* Each of them will need to pass a control procedure in order to determine the frequency response of each pixel, its sensitivity, to detect bad pixels, to calibrate the grating position with wavelength and so on. Also it needs to be checked the matching between the original specifications and the real characteristics of the detectors and the data acquisition electronics.

This set of measurements - identified with the term *calibration* - will be performed in collaboration between the **Max-Planck-Institut für Extraterrestrische Physik (MPE)** of Garching, (Germany) and three groups from Florence, namely the **Osservatorio Astrofisico di Arcetri (OAA)**, the **Istituto di Radioastronomia (IRA-CNR)**

Sez. di Firenze and the **Laboratorio Europeo di Spettroscopia non-lineare (LENS)**.

To perform the calibration a monochromatic beam of radiation, tunable along the whole range $60 \div 210 \mu m$, will be used. The beam will be produce by a special instrument called TuFIR (TuFIR = Tunable Far InfraRed spectrometer) developped by LENS [1], [2].

The spectrometer produces FIR (Far InfraRed) radiation by mixing over a MIM (metal-insulator-metal) diode the radiation (of different wavelength) emitted by two CO_2 lasers.

The lasers are frequency stabilized by an electronic feedback, using a saturated fluorescence signal from two cells containing low pressure CO_2 gas.

The laser cavities are closed by two gratings in Littrow configuration which allow to select the emitting frequency.

The beams from the two lasers are overlapped by using a beam splitter and focused over a MIM diode with a $ZnSe$ lens.

The MIM diode, directly built in the laboratory, it's composed by a junction between an electrochemically deposited Tungsten tip and a polished nickel base.

The diode acts as a second order non-linear element by mixing the radiation from the two CO_2 lasers and re-emitting radiation - as a dipole antenna - at the difference frequency: $\nu_{FIR} = \nu_1 - \nu_2$ (where ν_1 e ν_2 are the two lasers frequences)

The FIR radiation is then collimated by locating the contact diode in the focus of a reflecting paraboloid.

The spectrometer TuFIR generates radiation in the spectral range $300GHz \div 6THz$ ($\lambda = 1mm \div 50 \mu m$) with an accuracy of about 50 kHz.

Typical radiated power is between 10 and 100 nW.

As schematically shown in fig. 1 the monochromatic beam produced by TuFIR will be splitted by a Beam Splitter located at 45° with respect to the beam direction and the secondary beams sent in turn to the instrument under examination (PACS) and to a power calibrated bolometer which will act as a reference detector.

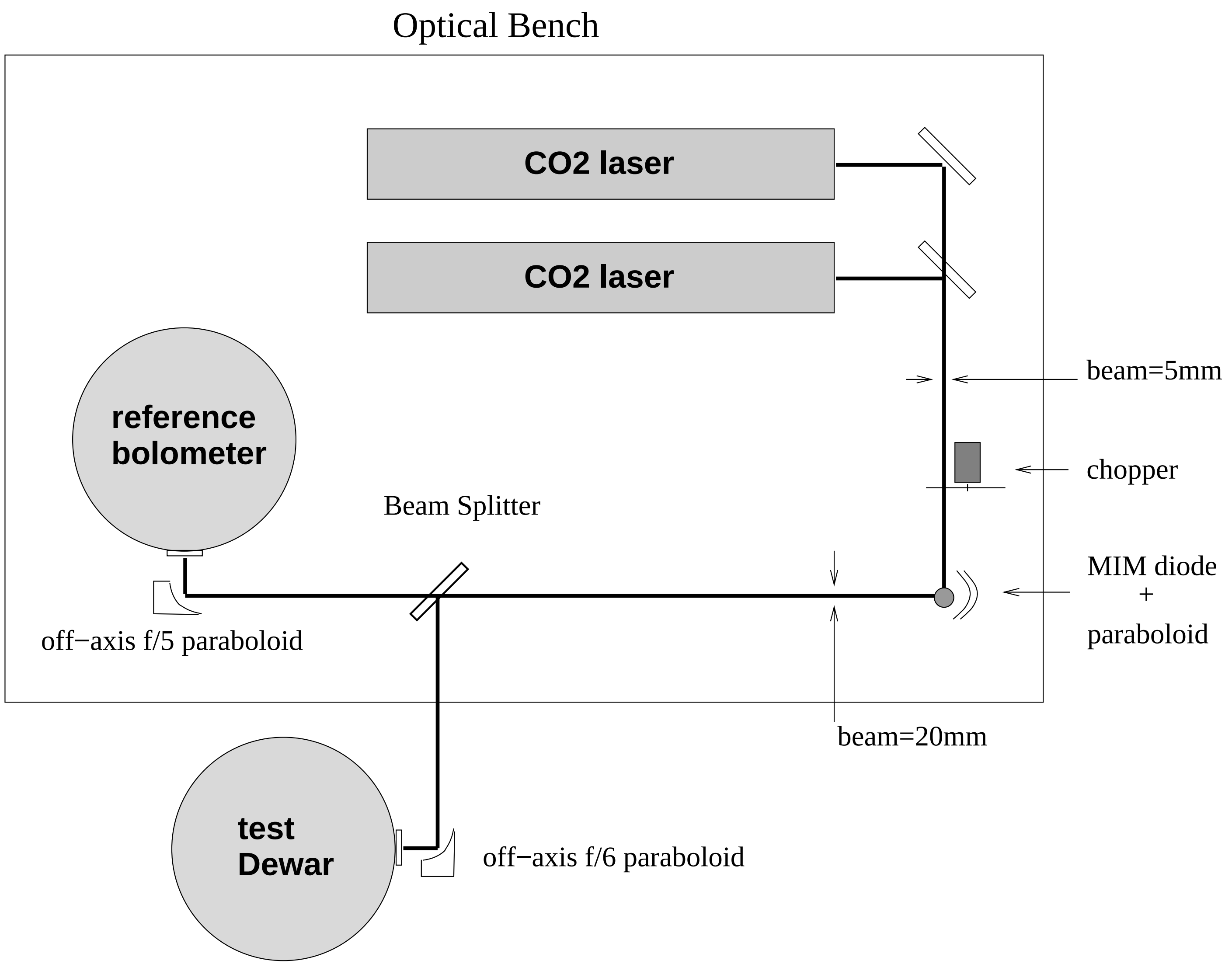

Figure 1: PACS calibration Setup

2 The Beam Splitter

Il Beam Splitter (BS) is an optical medium located along the path of a radiation beam with the purpose to separate the beam in two components, transmitted and reflected, which are in turn sent along different optical paths.

A BS is usually achieved by stretching between two rings a thin film of a material with good transmission/reflection coefficients on the wavelength range of interest. It is important that the two rings are designed in such a way to uniformely stretch the film, in order to produce a perfectly optically plane surface with no wrinkles.

Our BS should have the following characteristics:

- High transmission/reflection coefficient in the band $60 \div 210 \mu m$
- Free of absorbing bands in the former wavelength interval
- A large diameter, not to make too critical the centering of the radiation beam

It has been shown impossible to purchase a BS with all the above characteristics. Either the working wavelength interval or the size and/or optical parameters were out of our specifications in all commercially available models.

The only one ready-made BS we found working in the $60 \div 210 \mu m$ range - from one of the biggest firm in the field - was built with a half-reflecting area and a non-standard mount partially obstructing the optical path, being specifically designed to be used in a Michelson interferometer sold by the same firm. Besides the diameter was just 5 cm, which made the useful optical area quite small (when located at $45°$ inclination with respect to the incident beam) and the centering of the beam extremely critical.

With all these considerations in mind we decided to try and manufacture by ourselves in our workshop a BS fulfilling our requests.

This required to provide the material with the right optical parameters and to build the mechanical frame supporting and stretching the film.

3 The transmission/reflection coefficients

As optical medium we have chosen mylar, commonly used in interferometers and relatively easy to find with the required tickness. Dielectric characteristics of this material are reported in the literature [3], [4].

Refraction index and tickness are the parameters which determine the optical behavior of mylar as a beam splitter. What we look for are the transmission/reflection coefficients as a function of wavelenght, tickness of the mylar film and of the incidence angle of the incoming radiation. We have followed the treatment of the dielectric film reported in *Born & Wolf* [5].

In the following we report for convenience of the reader the adopted formulas as found on chapter 1.5 and 1.6 of the cited text. For an explanation of symbols we refer to the same text and especially to fig. 2

We define the angle $\beta = \frac{2\pi}{\lambda} n_2 h \cos\theta_2$

and identify with indexes $_{\parallel}$ and $_{\perp}$ the radiation with polarization plane respectively parallel and perpendicular to the incident plane.

Following *Born & Wolf* we obtain

$$\text{TE wave}\quad\left\{\begin{aligned}
r_{12} &= \frac{n_1\cos\theta_1 - n_2\cos\theta_2}{n_1\cos\theta_1 + n_2\cos\theta_2}\\
t_{12} &= \frac{2n_1\cos\theta_1}{n_1\cos\theta_1 + n_2\cos\theta_2}\\
r_{23} &= \frac{n_2\cos\theta_2 - n_3\cos\theta_3}{n_2\cos\theta_2 + n_3\cos\theta_3}\\
t_{23} &= \frac{2n_2\cos\theta_2}{n_2\cos\theta_2 + n_3\cos\theta_3}\\
\mathcal{R}_\perp &= \frac{r_{12}^2 + r_{23}^2 + 2r_{12}r_{23}\cos 2\beta}{1 + r_{12}^2 r_{23}^2 + 2r_{12}r_{23}\cos 2\beta}\\
\mathcal{T}_\perp &= \frac{n_3\cos\theta_3}{n_1\cos\theta_1}\frac{t_{12}^2 t_{23}^2}{1 + r_{12}^2 r_{23}^2 + 2r_{12}r_{23}\cos 2\beta}
\end{aligned}\right.$$

$$\text{TM wave}\quad\left\{\begin{aligned}
r_{12} &= \frac{n_2\cos\theta_1 - n_1\cos\theta_2}{n_1\cos\theta_1 + n_2\cos\theta_2}\\
t_{12} &= \frac{2n_1\cos\theta_1}{n_2\cos\theta_1 + n_1\cos\theta_2}\\
r_{23} &= \frac{n_3\cos\theta_2 - n_2\cos\theta_3}{n_3\cos\theta_2 + n_2\cos\theta_3}\\
t_{23} &= \frac{2n_2\cos\theta_2}{n_3\cos\theta_2 + n_2\cos\theta_3}\\
\mathcal{R}_\parallel &= \frac{r_{12}^2 + r_{23}^2 + 2r_{12}r_{23}\cos 2\beta}{1 + r_{12}^2 r_{23}^2 + 2r_{12}r_{23}\cos 2\beta}\\
\mathcal{T}_\parallel &= \frac{n_3\cos\theta_3}{n_1\cos\theta_1}\frac{t_{12}^2 t_{23}^2}{1 + r_{12}^2 r_{23}^2 + 2r_{12}r_{23}\cos 2\beta}
\end{aligned}\right.$$

In the calculation we do not take into account the mylar absorption - of negligeble amount for our purposes - in the $60 \div 210 \mu m$ band, cfr. [3].

The following relations hold

$$\begin{aligned} \mathcal{R}_{\perp} + \mathcal{T}_{\perp} &= 1 \\ \mathcal{R}_{\parallel} + \mathcal{T}_{\parallel} &= 1 \end{aligned}$$

We have no information concerning the polarization of the incident radiation. Assuming that energy is distribuited in the same amount between the two polarization planes we defin the transmission and reflection coefficients as follows:

$$\begin{aligned} \mathcal{R} &= \frac{\mathcal{R}_{\perp} + \mathcal{R}_{\parallel}}{2} \\ \mathcal{T} &= \frac{\mathcal{T}_{\perp} + \mathcal{T}_{\parallel}}{2} \end{aligned}$$

We applied the formulas just described to write a computer program to calculate - from 50 μm to 250 μm with 1 μm resolution - the coefficients $\mathcal{T}$ e $\mathcal{R}$ for several mylar tickness commercially available (12, 19, 23, 36, 50 and 100 μm) in order to identify the most appropriate one. The result is shown in graphics from fig. 3 to fig. 8.

From a look to these plots we have reached the conclusion that mylar with tickness 12 μm and 19 μm are well fit to be used as a film in a BS in the spectral range of interest, showing a reasonable uniform behavior for the transmission and reflection coefficients.

Worth to be noted is that the reflection coefficient never gets too close to zero, as instead it happens for the ticker film.

Besides, with just one single tickness we are able to cover the full spectral range $50 \div 250 \mu m$, which lessens the probability of perturbing the measurement apparatus and help to obtain homogeneous readings in the whole band.

Finally, taking into account its greater mechanical stiffness and robustness, we have selected the 19 μm tickness film as the one of choice for our BS.

4 Incidence angle $\neq 45°$

The result of the calculations shown in figures $3 \div 8$ refers to a configuration with 45° for the incidence angle of the radiation. This choice is the easiest to accomodate the several components of our calibration setup. Nevertheless it could be interesting to check the result when the incidence angle has a different value than 45°, especially a higher one.

We have repeated the calculation for incidence angles of 60° and 75°. The result is shown - only for tickness of $12\mu m$ and $19\mu m$ - in figures $9 \div 12$. We notice that the transmission coefficient is lower - and consequently higher the one for reflection - for a higher incident angle. The *passband* (limited by the reflection coefficient for a incident angle of 45°) is then greater.

In our case this would allow to use our BS beyond $\simeq 50\mu m$ and $\simeq 250\mu m$, even if it should be taken into account the drawback of a reduced surface.

5 Mechanical building

The Beam Splitter is composed by two aluminium rings (one of which with the internal rim smoothed) through which a mylar film is stretched. The two rings are linked together by three screws. By acting over them we can stretch the mylar to obtain a perfectly flat optical surface.

The BS final look is shown in fig. 13 and 14.

References

[1] K.M. Evenson, D.A. Jennings, and F. R. Petersen, Appl. Phys. Lett. 44, 576 (1984).

[2] L. R. Zink, P. De Natale, F. S. Pavone, M. Prevedelli, K. M. Evenson, and M. Inguscio, J. Mol. Spectrosc. 143, 304, (1990).

[3] Donald R. Smith and Ernest V. Loewenstein *Optical Constants of Far Infrared Materials. 3: plastics* Applied Optics, 1975, Vol. 14, No 6.

[4] Donald R. Smith and Ernest V. Loewenstein *Far-Infrared thin-film beam splitters: calculated properties* Applied Optics, 1975, Vol. 14, No 10.

[5] Born & Wolf *Principles of Optics* Second Edition, 1964, Pergamon Press.

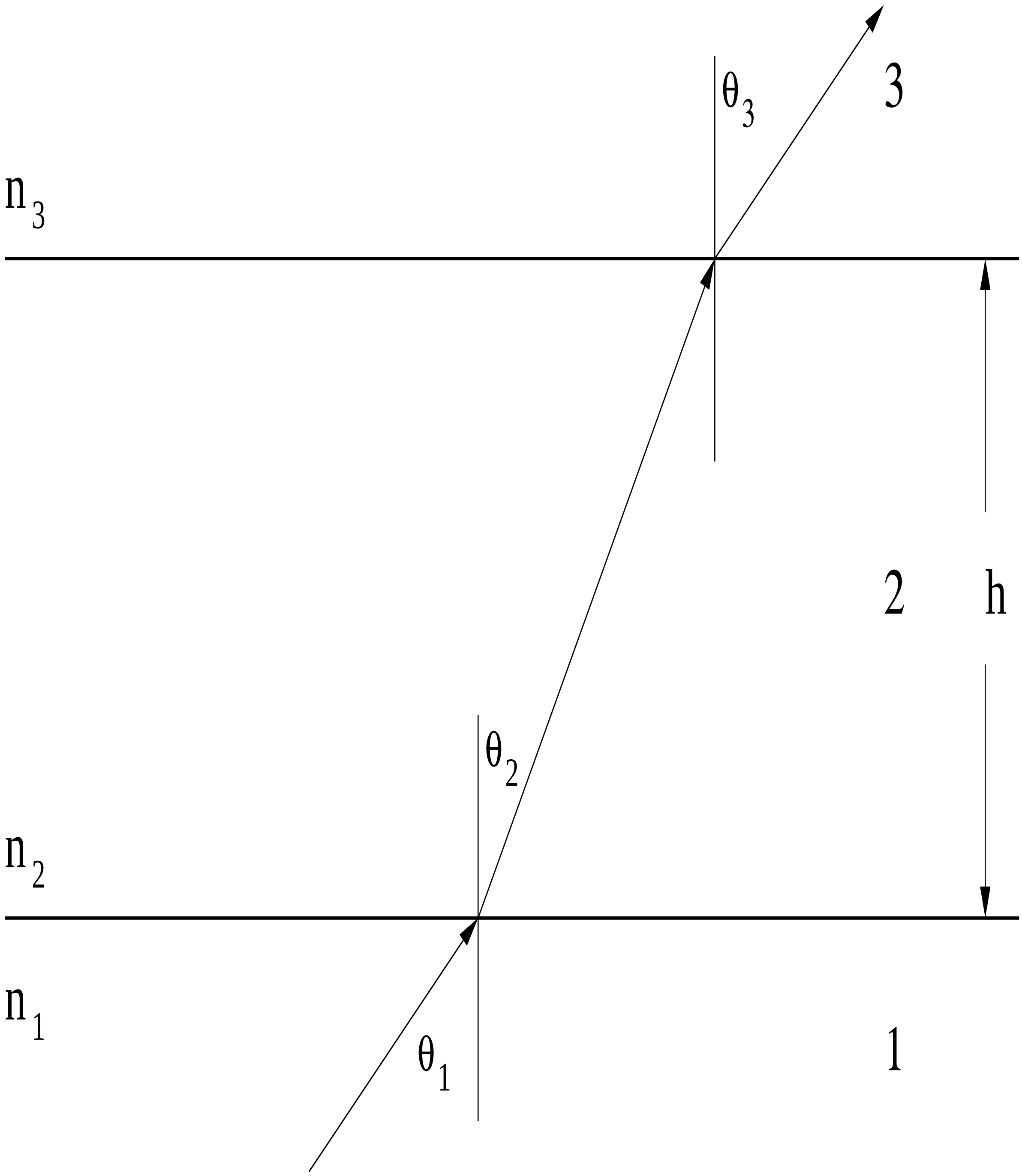

Figure 2: Electromagnetic wave propagation in homogeneous film

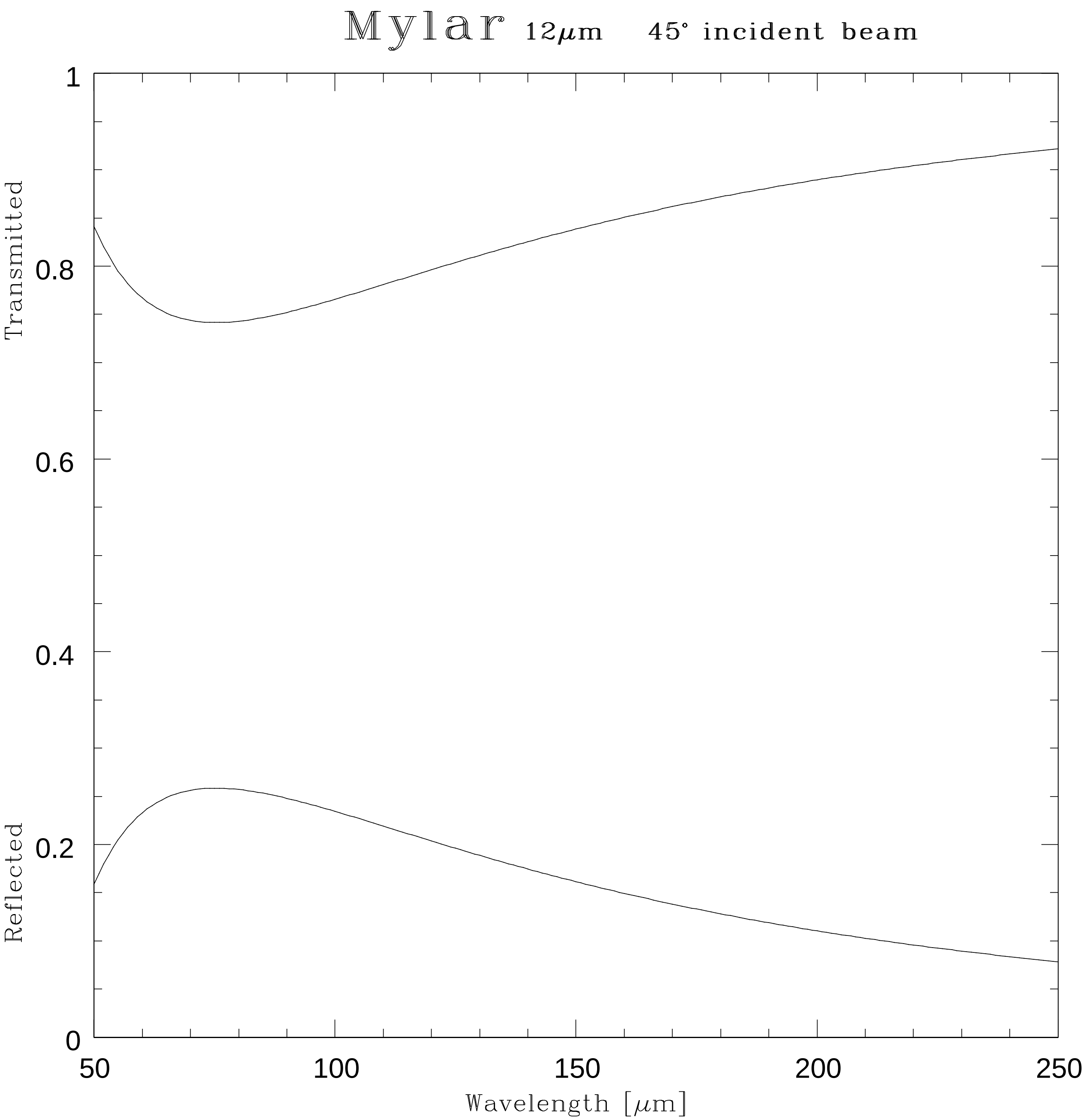
Mylar 12μm 45° incident beam
1
0.8
0.6
0.4
0.2
0
Transmitted
Reflected
50
100
150
200
250
Wavelength [μm]

Figure 3:

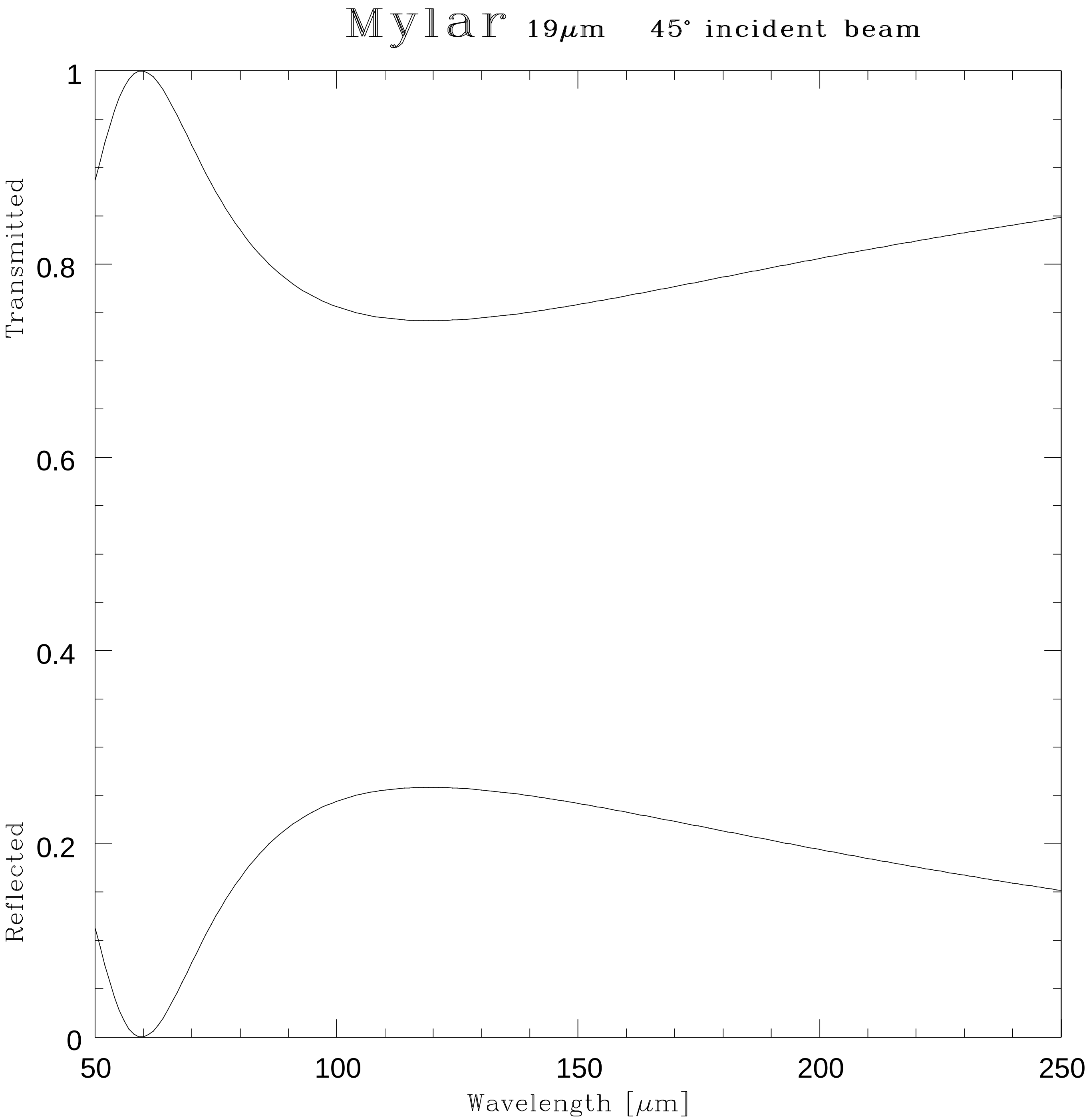
Mylar 19μm 45° incident beam
Transmitted
Reflected
1
0.8
0.6
0.4
0.2
0
50
100
150
200
250
Wavelength [μm]

Figure 4:

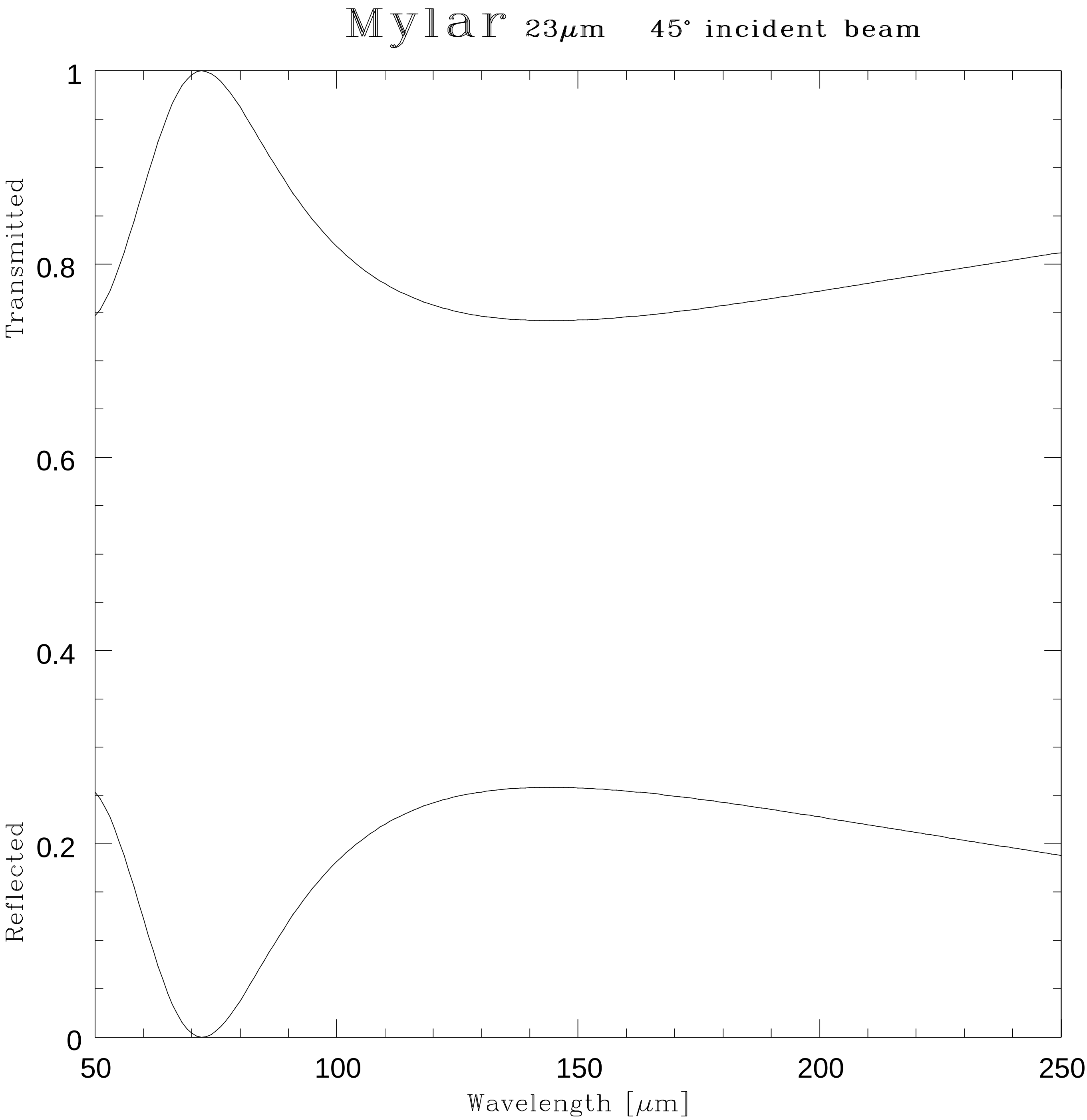
Mylar 23μm 45° incident beam
Transmitted
Reflected
1
0.8
0.6
0.4
0.2
0
50
100
150
200
250
Wavelength [μm]

Figure 5:

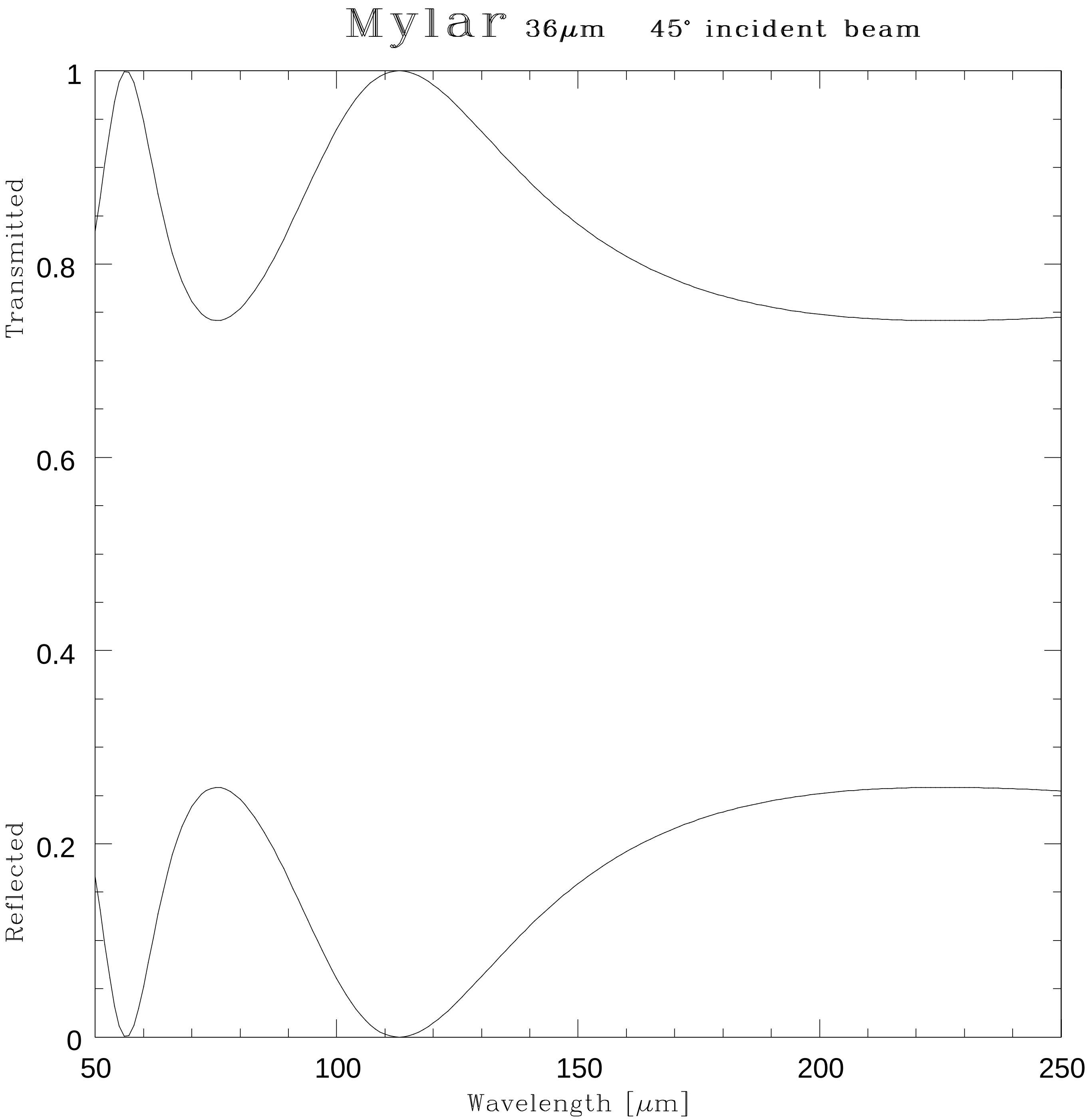
Mylar 36μm 45° incident beam
Transmitted
Reflected
1
0.8
0.6
0.4
0.2
0
50
100
150
200
250
Wavelength [μm]

Figure 6:

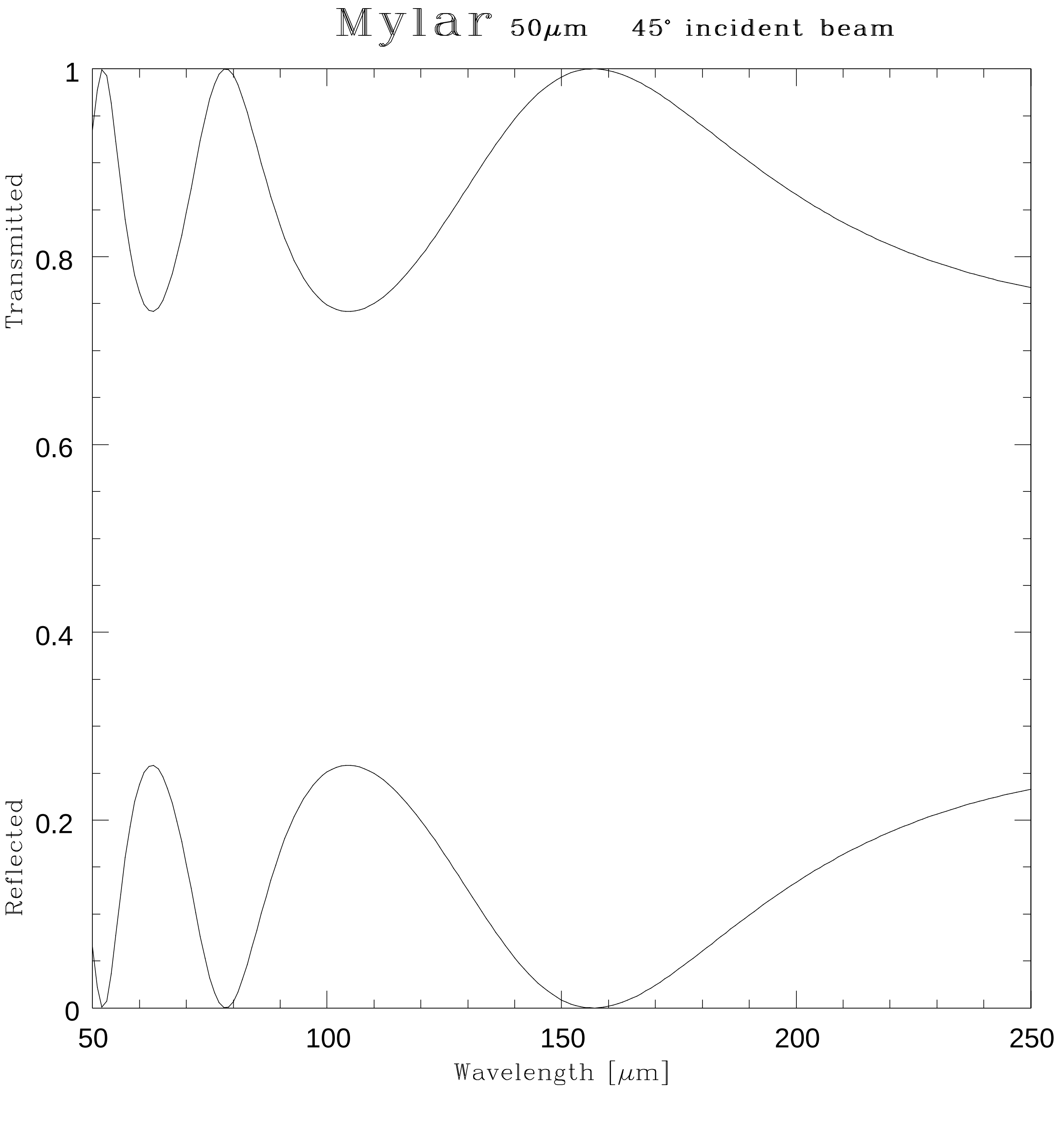
Mylar 50μm 45° incident beam
Transmitted
Reflected
1
0.8
0.6
0.4
0.2
0
50
100
150
200
250
Wavelength [μm]

Figure 7:

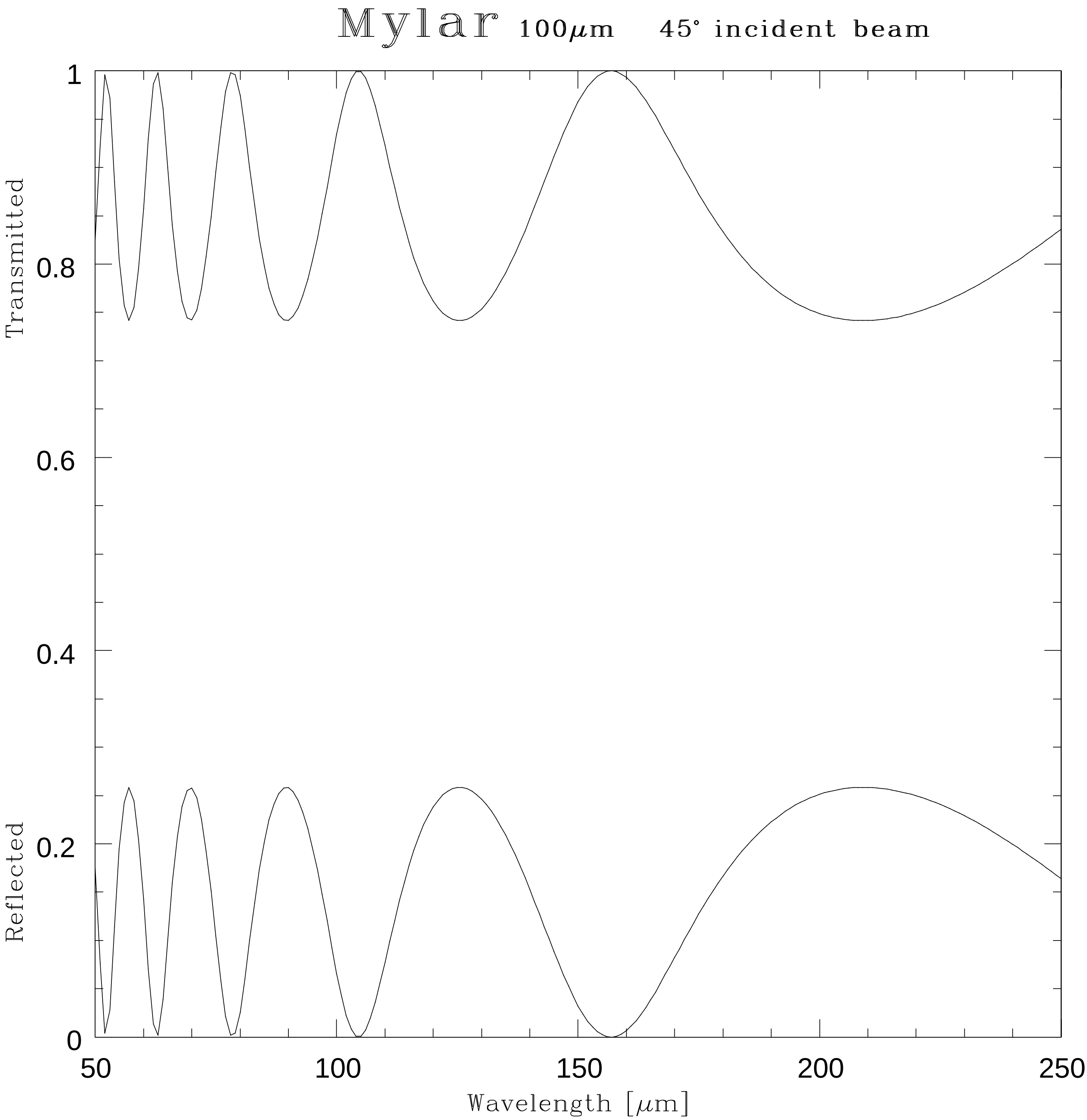

Mylar 100μm 45° incident beam
Transmitted
Reflected
Wavelength [μm]
0
0.2
0.4
0.6
0.8
1
50
100
150
200
250

Figure 8:

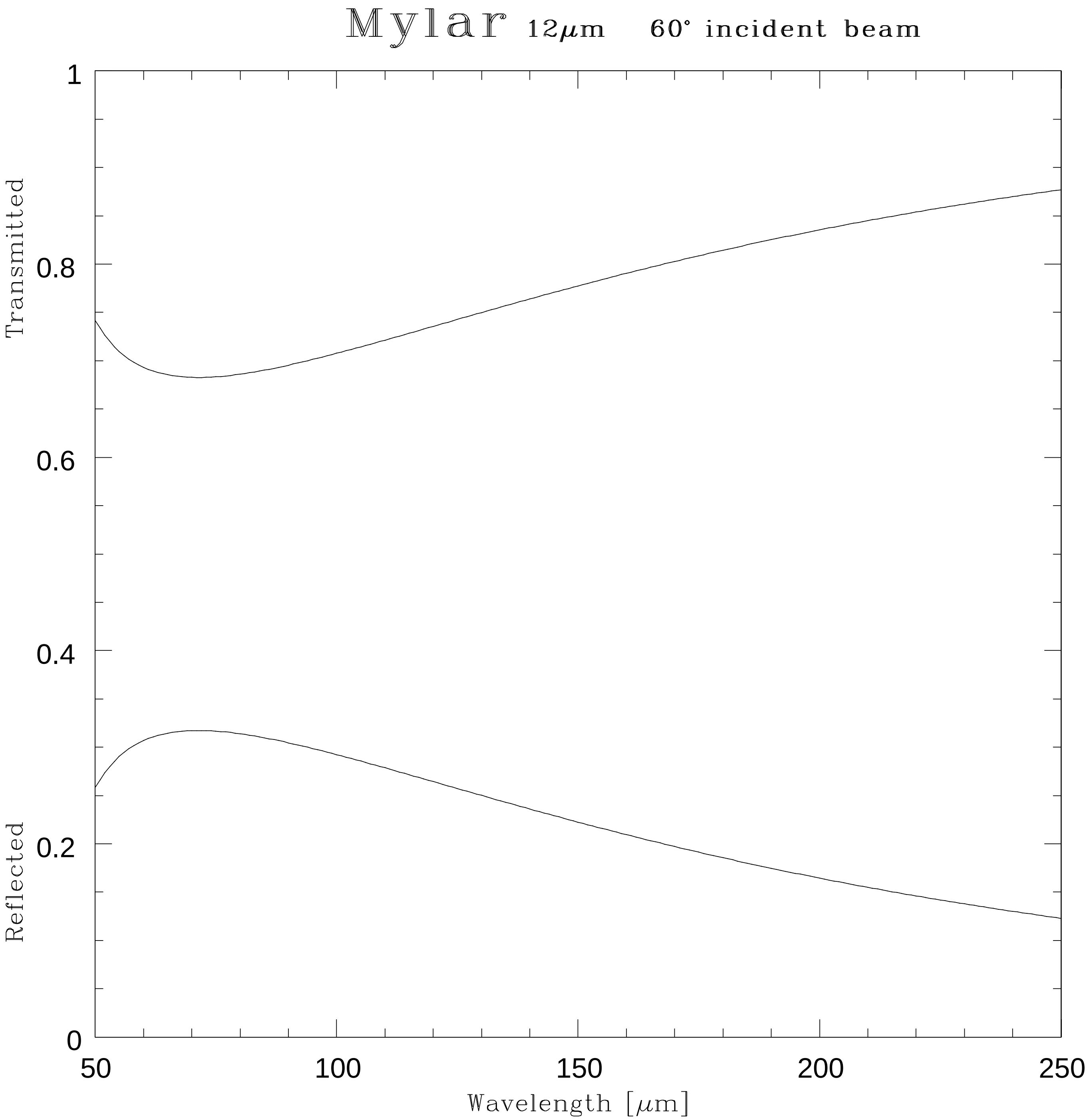
Mylar 12μm 60° incident beam
1
0.8
0.6
0.4
0.2
0
Transmitted
Reflected
50
100
150
200
250
Wavelength [μm]

Figure 9:

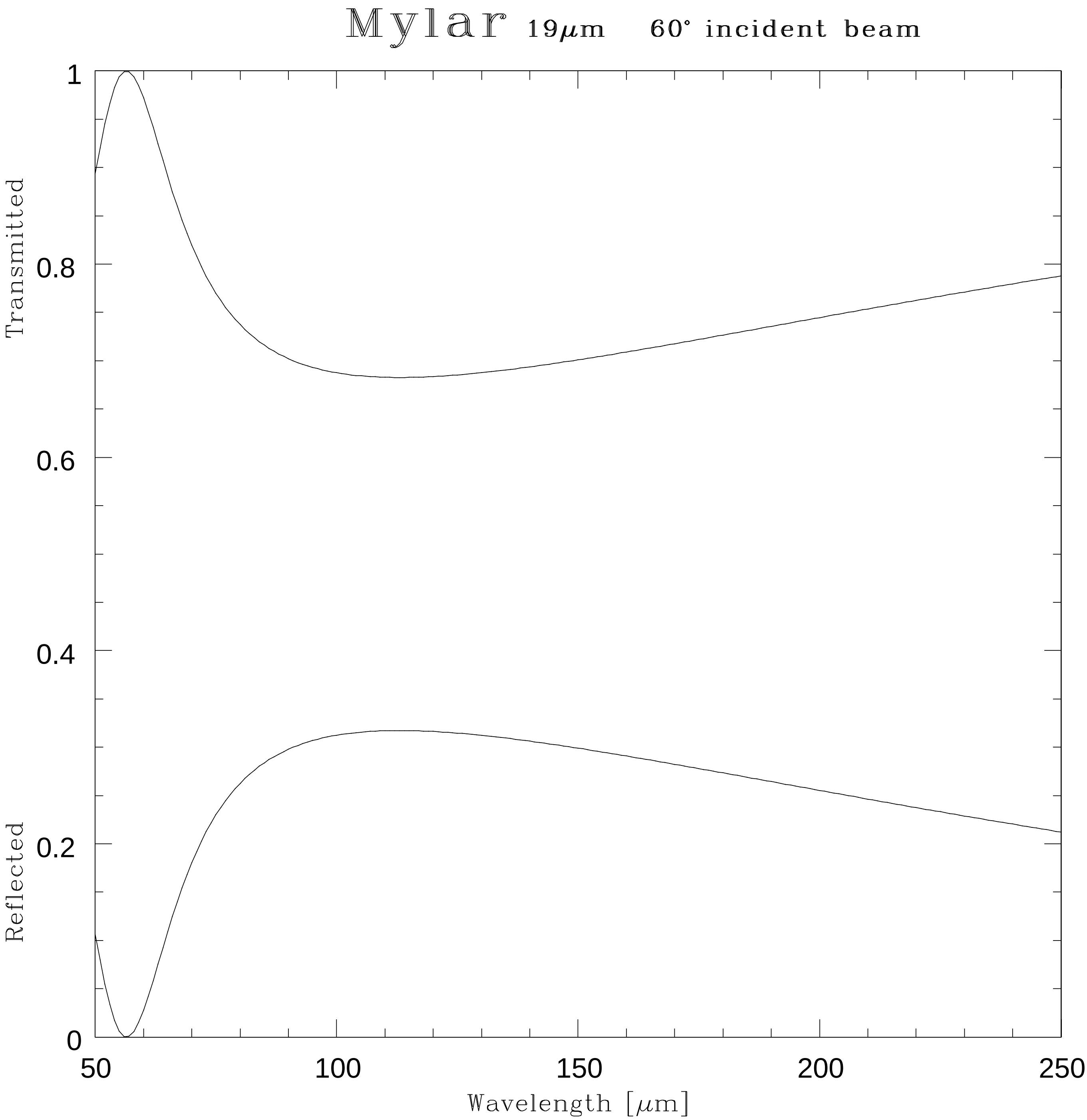
Mylar 19μm 60° incident beam
Transmitted
Reflected
1
0.8
0.6
0.4
0.2
0
50
100
150
200
250
Wavelength [μm]

Figure 10:

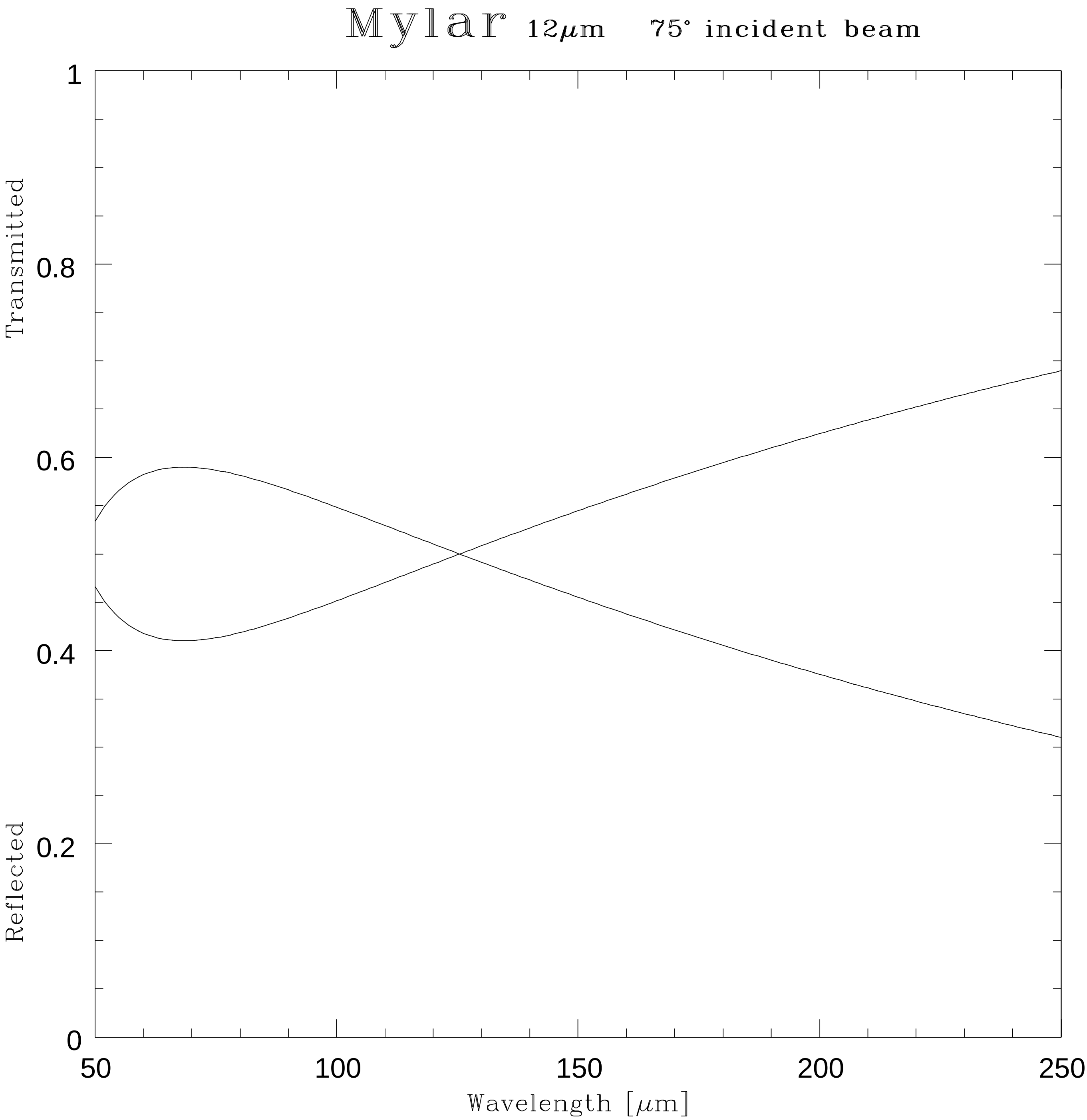
Mylar 12μm 75° incident beam
Transmitted
Reflected
Wavelength [μm]
0
0.2
0.4
0.6
0.8
1
50
100
150
200
250

Figure 11:

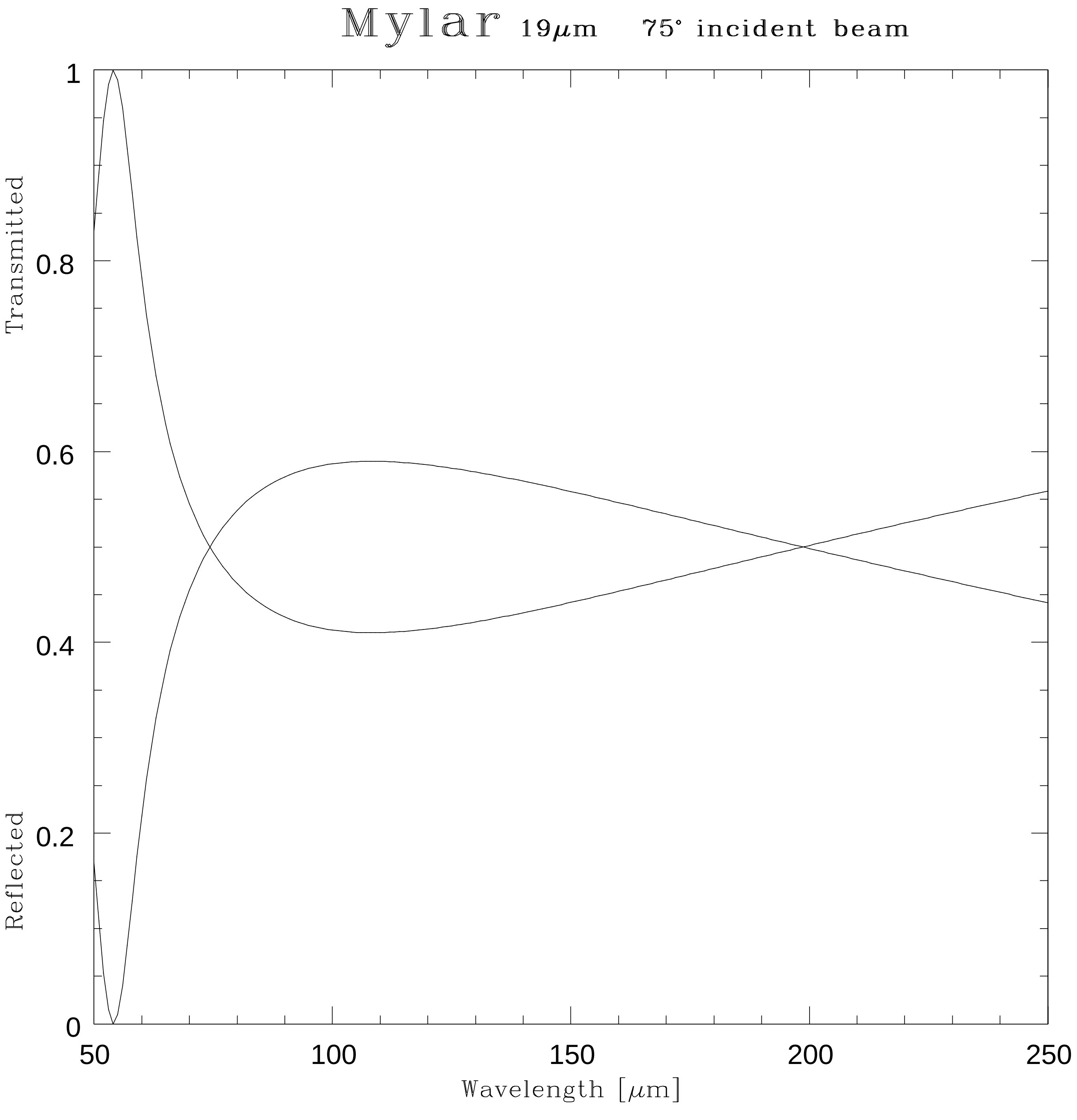
Mylar 19μm 75° incident beam
Transmitted
Reflected
1
0.8
0.6
0.4
0.2
0
50
100
150
200
250
Wavelength [μm]

Figure 12:

Figure 13: Beam Splitter - front view

Figure 14: Beam Splitter - back view